Lab on a Chip

Accepted Manuscript

RSC Publishing

www.rsc.org/loc

Registered Charity Number 207890

Title:

Microfabricated perfusable cardiac biowire: a platform that mimics native cardiac bundle

Yun Xiao[a,c], Boyang Zhang[a,c], Haijiao Liu[b,c], Jason W. Miklas[c], Mark Gagliardi[d], Aric Pahnke[a,c], Nimalan Thavandiran[a,c], Yu Sun[b,c], Craig Simmons[b,c], Gordon Keller[d], Milica Radisic[a,c *]

Author affiliations:

[a]Department of Chemical Engineering and Applied Chemistry, University of Toronto, Toronto, ON, Canada

[b]Department of Mechanical and Industrial Engineering, University of Toronto, Toronto, ON, Canada

[c]Institute of Biomaterials and Biomedical Engineering, University of Toronto, Toronto, ON, Canada

[d]McEwen Centre for Regenerative Medicine, University Health Network, Toronto, Ontario, Canada

Correspondence to:

[*]164 College St, Rm 407 Toronto, ON, M5S 3G9, m.radisic@utoronto.ca

Abstract

Tissue engineering enables the generation of three-dimensional (3D) functional cardiac tissue for pre-clinical testing *in vitro*, which is critical for new drug development. However, current tissue engineering methods poorly recapitulate the architecture of oriented cardiac bundles with supporting capillaries. In this study, we designed a microfabricated bioreactor to generate 3D micro-tissues, termed biowires, using both primary neonatal rat cardiomyocytes and human embryonic stem cell (hESC) derived cardiomyocytes. Perfusable cardiac biowires were generated with polytetrafluoroethylene (PTFE) tubing template, and were integrated with electrical field stimulation using carbon rod electrodes. To demonstrate the feasibility of this platform for pharmaceutical testing, nitric oxide (NO) was released from perfused sodium nitroprusside (SNP) solution and diffused through the tubing. The NO treatment slowed down the spontaneous beating of cardiac biowires based on hESC derived cardiomyocytes and degraded the myofibrillar cytoskeleton of the cardiomyocytes within the biowires. The biowires were also integrated with electrical stimulation using carbon rod electrodes to further improve phenotype of cardiomyocytes, as indicated by organized contractile apparatus, higher Young`s modulus, and improved electrical properties. This microfabricated platform provides a unique opportunity to assess pharmacological effects on cardiac tissue *in vitro* by perfusion in a cardiac bundle model, which could provide improved physiological relevance.

1. Introduction

Cardiovascular diseases are important targets for pharmacological therapy because they are associated with high morbidity and mortality rates[1]. *In vitro* engineered models may serve as cost-effective alternatives to animal models due to improved system control and higher throughput. In recent years, tissue engineering methods have been significantly advanced to generate functional three-dimensional (3D) cardiac tissues *in vitro*[2–4], which better recapitulate the complexity and electro-mechanical function of native myocardium compared to conventional *in vitro* systems of single cell suspensions or monolayers. Moreover, with the opportunities brought about by human pluripotent stem cells (hPSC), tissue engineering methods hold a great promise in developing patient-specific medical treatment[5].

In native myocardium, cardiomyocytes are highly anisotropic, usually in a length of 80-100 μm and 20-30 μm in diameter[6]. Each cardiomyocyte adjoins neighboring cardiomyocytes by specialized intracellular junctions, such as gap junctions and desmosomes, to form a complex 3D network, or syncytium. On tissue level, native cardiomyocytes are organized into spatially well-defined cardiac bundles with supporting vasculature. This highly organized architecture is critical for electro-mechanical activation, propagation of electrical signals, and global cardiac function[7]. Cardiac tissues generated by current tissue engineering methods often poorly recapitulate this architecture.

Increased cardiovascular risk is one of the major unwanted side effects of new drug

candidates, which frequently leads to usage restriction or even withdrawal from the market[8]. Cardiac toxicity was the main reason behind withdrawal of numerous drugs from the market, including well known examples such as Vioxx or Avanida, accounting for up to 20% of all drug withdrawals[9,10]. Thus, it is essential to identify these risks at an early stage in drug development process to define safety profile and avoid cost escalation. Despite the exceptional progress in developing cardiac disease models with hPSC (Timothy[11], long QT[12], LEOPARD syndrome[13] and dilated cardiomyopathy patients[14]), most studies still use cardiac monolayers that do not capture architectural complexity of the native cardiac niche. After pharmacologic agents are administrated into human body, they are circulated through the vasculature and delivered to the myocardium by the blood in capillaries. Current *in vitro* drug testing systems, however, expose the cardiac cells to the pharmacologic agents directly from the culture media in conventional well plates[15–18]. Thus, developing *in vitro* cardiac systems that can recapitulate the perfusion scenario could provide improved physiological relevance when assessing pharmacological effects on cardiac tissue *in vitro*.

We recently described a development of a human cardiac micro-tissue, termed biological wire, which captures some of the architectural complexity of the native myocardium and enables maturation of cardiomyocytes derived from human pluripotent stem cells with the application of electrical stimulation[19]. However, these original biowires lacked perfusion, a critical aspect for mimicking native physiology and mass transfer. We describe here technological developments required to create a

perfusable biowire conducive to electrical field stimulation and we prove the feasibility of drug testing in this system.

Perfusable cardiac biowires were generated using a polytetrafluoroethylene (PTFE) tubing template in microfabricated bioreactors, which provided contact guidance for cells to align and elongate. To demonstrate the feasibility of this platform for drug testing, we supplied nitric oxide (NO) in the cell culture channel to provide biochemical stimulation to cardiomyocytes within the biowire. NO was released from perfused sodium nitroprusside (SNP) solution and passed through the tubing wall to reach the tissue constructs with cardiomyocytes. This bioreactor was also integrated with electrical stimulation to further improve phenotype of cardiomyocytes.

2. Materials and methods

2.1 Biowire bioreactor design and fabrication

The biowire bioreactor consisted of two main units, the microfabricated platform made of poly(dimethysiloxane) (PDMS) and the suspended template made of either silk 6-0 suture or Polytetrafluoroethylene (PTFE) micro-tubing. To fabricate the PDMS platform, standard soft lithography technique was used to make to a two-layer SU-8 (Microchem Corp., Newton, MA) master[20]. The first layer included the template channel and the cell culture chamber, while second layer included only the cell culture chamber. Then PDMS was cast onto the SU-8 master and baked for 2 hr at 70 °C. A biowire template was then anchored to the two ends of the PDMS platform followed by the bioreactor sterilization in 70% ethanol and overnight UV irradiation.

2.2 Perfusion system design and fabrication

In order to provide perfusion through the tubing template, two microfabricated modules, drug reservoir and connecting channel, were added to the biowire bioreactor. Both modules were fabricated by first molding PDMS with a single-layer SU-8 master (length × width × height = 10 × 1 × 0.3 mm). The drug reservoir was created by cutting through the PDMS using an 8 mm biopsy punch (Sklar). The biowire bioreactor channel was connected to the drug reservoir and connecting channel with the PTFE tubing (inner diameter (ID) = 0.002 inch, outer diameter (OD) = 0.006 inch, Zeus)**.** Tygon tubing (ID = 0.01 inch, OD = 0.03 inch, Thomas Scientific) connected the perfusion system to external negative pressure generated by a peristaltic pump. The perfusion rate was characterized by the liquid volume collected at the outlet from the peristaltic pump (n = 3). All the connecting points were secured by epoxy glue and three microfabricated modules were plasma bonded to a glass slide**.**

2.3 Cell culture

Neonatal rat cardiomyocytes were obtained from 2-day old neonatal Sprague-Dawley rats as described previously[21] and according to a protocol approved by the University of Toronto Committee on Animal Care. The culture media contained 10% (v/v) fetal bovine serum, 1% (4-(2-hydroxyethyl)-1-piperazineethanesulfonic acid) (HEPES), 100 U/ml penicillin-streptomycin, 1% Glutamine, and the remainder Dulbecco`s modified Eagle`s medium.

Cardiac differentiation in embryoid bodies (EBs) of HES-2 human embryonic stem

cell (hESC) line was performed as described previously[22,23]. Briefly, EBs were first cultured in StemPro-34 (Invitrogen) media containing BMP4 (1 ng/ml). On day 1, they were transferred to the induction medium (StemPro-34, basic fibroblast growth factor (bFGF; 2.5 ng/ml), activin A (6 ng/ml) and BMP4 (10 ng/ml)). On day 4, the EBs were removed from the induction medium and re-cultured in StemPro-34 supplemented with vascular endothelial growth factor (VEGF; 10 ng/ml) and Inhibitor of Wnt production-2 (IWP2; 2 μM). On day 8, the medium was changed again and the EBs were cultured in StemPro-34 containing VEGF (20 ng/ml) and bFGF (10 ng/ml) for the remainder of EB culture as well as for the biowire culture. EBs were maintained in hypoxic environment (5% CO_2, 5% O_2) for the first 12 days and then transferred into a 5% CO_2 for the remainder of the culture period. EBs were dissociated for seeding in biowires at day 23 (EBd23).

2.4 Generation of cardiac biowires

Cardiac cells (from neonatal rat isolation or hESC differentiation) were first suspended at 200 million /ml (unless specified otherwise) in Collagen Type I based gel (2.5 mg/ml of rat tail collagen type I (BD Biosciences) neutralized by 1N NaOH and 10× M199 media as described by the manufacturer) with the supplements of 4.5 μg/ml glucose, 1% (v/v) HEPES, 10% (v/v) Matrigel (BD Biosciences), and 2 μg/ml $NaHCO_3$. Suspended cardiac cells were then seeded into the cell culture channel (3 μl per biowire). After 30 min incubation at 37 °C to induce the gelation, appropriate media were added. Cardiac biowires were kept in culture for up to 14 days with media

change every 2-3 days.

Cardiac biowires starting with different cell densities (100 and 200 million/ml) were seeded to study the effect of the cell seeding density. Collagen-based gel was seeded into the cell culture channel without loading cardiac cells, to serve as a cell-free control. Ultra-long cardiac biowires were generated with customized biowire bioreactor that was 5 cm long fabricated in a similar manner as described above and seeded with neonatal rat cardiomyocytes.

2.5 Quantification of compaction rate

After seeding, brightfield images of the biowires were taken every day (n = 3 per group) using an optical microscope (Olympus CKX41) and the diameters of the biowires at five distinct locations were averaged with image analysis.

2.6 Immunostaining and Fluorescent Microscopy

Biowires were fixed with 4% paraformaldehyde, permeablized by 0.25% Triton X-100, and blocked by 10% bovine serum albumin (BSA). Immunostaining was performed using the following antibodies: mouse anti-cardiac Troponin T (cTnT) (Abcam; 1:100), rabbit anti-Connexin 43 (Cx-43) (Abcam; 1:200), mouse anti-α-actinin (Abcam; 1:200), goat anti-mouse-Alexa Fluor 488 (Jackson Immuno Research; 1:400), anti-rabbit-TRITC (Invitrogen; 1:200), anti-mouse-TRITC (Jackson Immuno Research; 1:200). Nuclei were counterstained with 4',6-diamidino-2-phenylindole (DAPI) (Biotium; 1:100). Phalloidin-Alexa 660

(Introgen; 1:600) was used to stain F-actin fibers. For confocal microscopy, the stained cardiac biowires were visualized under an inverted confocal microscope (Olympus IX81) or an upright confocal microscope (Zeiss LSM 510).

2.7 Quantification of nuclei elongation and alignment

Cell nuclei within the biowires were visualized by DAPI staining and z-stack images were obtained by confocal microscopy with 3 μm interval. Each stack of the confocal images was analyzed in ImageJ 1.45s (National Institutes of Health, USA) with an automated algorithm described by Xu et al[24] with approximately 1000 nuclei analyzed per sample. Nuclei elongations were characterized as nucleus aspect ratios, the ratio of long axis over short axis of the nuclei, and nuclear alignment was characterized by orientation angles. In the control monolayer group, orientation of the nuclei was characterized compared to an arbitrarily defined orientation, while in the biowire group, the orientation of the suture templates was set as reference.

2.8 Characterization of perfusable biowires

Neonatal rat cardiac cells were seeded into the perfusable biowire reactors with tubing template. After cultivation for 7 days, the cardiac biowires were sectioned and visualized under environmental SEM (Hitachi S-3400 N). The biowires were imaged under variable pressure mode at 70 Pa and 15 kV and the chamber temperature was −20°C.

To visualize the cross-section, perfusable cardiac biowires were stained with cTnT antibody and then TRITC. Stained biowires were then cryo-sectioned into 500 μm

thick sections using a cryostat (Leica CM3050S) and mounted to Superfrost Plus glass slide (VWR). Images of the cross-sectioned biowires were acquired by Olympus fluorescent microscope (Olympus IX81).

To demonstrate the feasibility of the perfusable biowire bioreactor, FITC-labeled polystyrene beads (Spherotech Inc.) were added into the drug reservoir and perfused through the rat cardiac biowire, while it beat spontaneously on day 8. Bright-field and fluorescent videos and images were acquired with a fluorescence microscope (Olympus IX81).

2.9 Quantification of NO perfusion

Sodium nitroprusside (SNP) (Sigma) was dissolved in distilled water to make 200 mM SNP solution and then added to the drug reservoir. Perfusion through the tubing template was driven by the external peristaltic pump. Once the SNP solution perfused through the tubing, the peristaltic pump was stopped and the entire perfusion system was kept in cell culture incubator. NO amount in the cell culture channel (outside the PTFE tubing) was quantified with a fluorometric Nitric Oxide Assay Kit (Calbiochem, 482655). In brief, samples collected from the cell culture channels (8 μl, n = 3) at different time points (0.5 hr, 6 hr, and 24 hr) were converted to nitrite by nitrate reductase and then developed into a fluorescent compound 1-H-naphthotriazole. The fluorescent signals were quantified by a plate reader (Apollo LB 911, Berthold Technologies) and compared to the nitrate standard.

2.10 NO treatment of human cardiac biowires

On day 7, the NO treatment of human cardiac biowire was initiated by perfusing the 200 mM SNP solution and the peristaltic pump was stopped once the SNP solution was perfused through the tubing. The beating activities of the human cardiac biowires were recorded at 16.67 frames/second before treatment and 24 hr post-treatment by Olympus IX81 while the biowires were kept at 37°C. The beating activities of the human cardiac biowires were quantified by the image analysis method described by Sage et al[25]. In brief, the movements of one spot at the same location on the human cardiac biowire before and after the NO treatment were characterized.

2.11 Electrical stimulation

Different electrical stimulation conditions were applied to the rat cardiac biowires as described previously[2]. The parallel stimulation chambers were fitted with two 1/4-inch-diameter carbon rods (Ladd Research Industries) placed 2 cm apart, perpendicular to the biowires (such that the electrical field was parallel with the biowire long axis), and connected to a stimulator (S88X, Grass) with platinum wires (Ladd Research Industries). The perpendicular stimulation chambers were built with two carbon rods 1 cm apart placed parallel with the biowires (i.e. the filed was perpendicular to the long axis of the biowire)**.** The biowires were pre-cultured for 4 days until the biowire structures were established and their spontaneous beating was synchronized, and then subjected to the electrical field stimulation (biphasic, rectangular, 1 ms duration, 1.2 Hz, 3.5-4 V/cm) for 4 days with 10 μM ascorbic acid supplemented in the culture media while control biowires were cultured without electrical stimulation. At the end of electrical stimulation, the rat cardiac biowires

were double stained for cTnT with Alexa 488 conjugated antibody and Cx-43 with TRITC conjugated antibody, or their mechanical properties were measured by atomic force microscopy (AFM). Confocal images were acquired using identical microscope settings for all groups. Areas stained positive for cTnT staining (green pixels) or Cx-43 staining (red pixels) were quantified by ImageJ using the identical thresholding parameters in all groups.

For the human perfusable cardiac biowire, only parallel electrical stimulation was applied as described above. Starting on day 4, electrical field stimulations (biphasic, rectangular, 1 ms duration, 1 Hz, 3.5-4 V/cm) were applied for 4 days while control biowires were cultured without electrical stimulation. Both stimulated and control biowires were perfused with culture medium at a flow rate of 2 μl/min within the PTFE tubing driven by an external syringe pump (PHD Ultra; Harvard Apparatus). At the end of electrical stimulation, the electrical properties of the stimulated and control human cardiac biowires were characterized in terms of excitation threshold (ET) and maximum capture rate (MCR) under external field pacing as previously described[26].

2.12 Atomic force microscopy (AFM)

After application of electrical stimulations for 4 days, rat cardiac biowires were tested using a commercial AFM (Bioscope Catalyst; Bruker) mounted on an inverted optical microscope (Nikon Eclipse-Ti). The force-indentation measurements were done with a spherical tip (radius = 5-10 μm) at nine distinct spots to evenly cover the center of the cardiac biowires with 5 nN trigger force at 1 Hz indentation rate. The cantilever

(MLCT-D, Bruker) had a nominal spring constant of 0.03 N/m. Hertz model was applied to the force curves to estimate the Young's modulus and detailed data analysis was described elsewhere[27]. All AFM measurements were done in fluid environment at room temperature.

2.13 Statistical analysis

Statistical analysis was performed using SigmaPlot 11.0. Differences between experimental groups were analyzed using t-test or one-way ANOVA with significant difference considered as $p < 0.05$.

3. Results

3.1 Generation and characterization of cardiac biowires

The native myocardium has a highly anisotropic structure (**Figure 1a**) with a high density of capillaries (**Figure 1b**) and surrounding elongated and aligned cells (**Figure 1c**). In the native heart, extracellular matrix (ECM) serves as a template for cells to align and elongate[28]. In addition, a structural correlation between directionality of capillaries and cardiomyocytes can be readily observed[6]. We aimed to emulate this in our biowire bioreactor by introducing a perfusable tubing template and by using a hydrogel, for cell seeding, consisting of ECM molecules normally present in the native heart. Primary neonatal rat cardiomyocytes were used to generate 3D, self-assembled cardiac biowires by seeding within type I collagen-based gel into microfabricated PDMS platforms with suspended templates **(Figure 2b)**. Seeded cells

remodeled and contracted the collagen gel matrix around the templates within a week **(Figure 2a, Figure 4a)**. The gel compaction only occurred with the presence of the seeded cells, as cell-free gels did not compact or degrade during the culture time, and the compaction rate positively correlated with the cell seeding density **(Figure 2d)**. Cardiac biowires of different dimensions could be generated by customizing the dimensions of the biowire bioreactor. Here, we generated biowires as long as 5 cm **(Figure 2c)**. Generation of longer biowires might be possible; however it was not explored in this work.

Image analysis of the cell nuclei that counterstained with DAPI **(Figure 3a, left)** revealed nuclei elongation and alignment along the axis of suture template. There was a significant difference ($p < 0.001$) of nuclei aspect ratio between biowires and monolayer group **(Figure 3b)**. Compared to neonatal rat cardiomyocytes cultured in monolayer controls, biowires had a lower frequency of cells in the smaller aspect ratio range and a higher frequency of cells in the larger aspect ratio range **(Figure 3c)**. Image analysis also revealed that cell nuclei in biowires were oriented along with the axis of the suture template, while those in monolayers were randomly distributed **(Figure 3d)**.

Neonatal rat cardiac biowires started to beat spontaneously between 3 and 4 days post-seeding and kept beating during gel compaction, demonstrating that the biowire bioreactor allowed for electromechanical coupling of the cells within the hydrogel matrix. The spontaneous beating of biowires with higher seeding density (200

million/ml) started earlier and was more prominent than in those with lower seeding density (100 million/ml) **(Video 1)**, which is thought to be a result of the presence of more cardiomyocytes and better coupling. Immunohistochemistry staining showed that the rat cardiac biowires expressed the sarcomeric protein, cTnT **(Figure 3a, right)**.

3.2 Generation and characterization of perfusable cardiac biowires

Primary neonatal rat and hESC-derived cardiomyocytes were used to generate perfusable cardiac biowires with PTFE tubing template **(Figure 4d)**. Both cell types were able to form the cardiac biowires and beat spontaneously **(Figure 4a, video 2, video 3, and video 4)**. As shown in SEM images, cells attached to the smooth surface of the PTFE tubing after self-remodeling **(Figure 4b)**. Cross sections of these perfusable biowires showed that self-remodeled cells encircled the tubing template and expressed cTnT **(Figure 4c)**.

The feasibility of perfusable biowire bioreactor was demonstrated by perfusion with FITC-labeled fluorescent beads. Perfusion rate driven by the peristaltic pump was quantified to be 2±0.16 μl/min (n = 3). Bright field video showed both spontaneous beating activity of the rat cardiac biowire and the perfusion of the fluorescent beads **(Video 2)**. The movement of the beads was better visualized under fluorescent view. A snapshot of the video **(Figure 4e)** was overexposed to provide better visualization of the fluorescent beads. The cardiac biowire was also visible in this image due to the auto-fluorescence of cardiomyocytes.

3.3 NO treatment of human cardiac biowires by perfusion

To demonstrate feasibility of drug testing in the perfusable cardiac biowire, a pharmacological agent, NO donor SNP, was applied to the culture media that was perfused through the tubing lumen. As NO was generated in the tubing lumen, it diffused through the tubing wall reaching the cell culture outer channel where the total amount of NO was quantified. The amount of NO released from 200 mM SNP was quantified by a fluorometric assay which validated the persistence of the NO release from SNP solution over several hours **(Figure 5a)**. The cumulative NO amount in the cell culture channel was 100 μM (800 pmol in 8μl), which exceeded the physiological levels of NO *in vivo*[29].

Upon gel compaction, the hESC-derived cardiomyocytes within the biowires started spontaneous beating **(Video 3 and Video 4)**. After NO treatment for 24 hr, performed by perfusion of NO-donor SNP through the tubing lumen, the spontaneous beating of human cardiac biowires slowed down **(Video 5)** and this was further characterized by image analysis **(Figure 5b, c)**. In order to compare beating frequency changes between different biowires, the frequencies after 24 hr NO treatment were normalized to the basal level (before treatment). The beating frequencies after NO treatment were significantly lower than the basal level (74±3%, n = 3) while the control biowires remained the same (100±9%, n = 3).

The degradation of cytoskeleton of cardiomyocytes within the biowires based on hESC derived cardiomyocytes caused by NO treatment through perfusion was

characterized using confocal microscopy for α-actinin labeled with Alexa 488 conjugated antibody (green) and actin labeled with Alexa 660 conjugated antibody (far red) **(Figure 5d)**. It was possible to clearly discern the striated pattern of sarcomeric Z-discs labeled with α-actinin in the control biowires, while the NO treated biowires showed an overall punctate pattern.

3.4 Electrical stimulation of cardiac biowires

To demonstrate the versatility of the cardiac biowire bioreactor, electrical stimulation was applied to further improve the phenotype of cardiomyocytes **(Figure 6a)**. Immunohistochemical staining showed that the rat cardiomyocytes in the biowires that underwent electrical stimulation with the field parallel to the biowire long axis had more cTnT positive structures oriented along with the axis of the suture template (indicated by the dashed line), while those in non-stimulated biowires were randomly distributed and those in perpendicular-stimulated biowires were found to be perpendicular to the suture template **(Figure 6b)**. Moreover, the cardiomyocytes in the parallel- and perpendicular- stimulated biowires showed stronger expression of Cx-43, a marker for the gap junctions between adjacent cardiomyocytes, compared to the control biowires, indicating better coupling between the cardiomyocytes in the stimulated groups (**Figure 6b**). This was also confirmed by comparing the ratio of Cx-43 positive area over cTnT positive area under same magnification with identical microscope settings (**Figure 6c**).

When handling the rat cardiac biowires outside the bioreactor, it was noticed that the

parallel-stimulated biowires were stiffer than the non-stimulated control. This was further assessed by AFM analysis (n = 3 per group), which revealed significantly (p = 0.009) improved mechanical properties of parallel-stimulated biowires compared to non-stimulated controls **(Figure 6d)**.

The perfusable human cardiac biowires that underwent medium perfusion through the tubing and parallel electrical stimulation at the same time showed improved electrical properties compared to the non-stimulated controls as assessed by ET and MCR under electrical field stimulation. The ET is the minimum electrical field voltage required for inducing synchronous contractions and the decreased ET of the stimulated biowires **(Figure 6e)** indicated better electrical excitability. The MCR is the maximum beating frequency attainable while maintaining synchronous contractions and the increased MCR **(Figure 6f)** of the stimulated biowires indicated improved cell alignment and interconnectivity.

4. Discussion

The native myocardium consists of spatially well-defined cardiac bundles with supporting vasculature **(Figure 1a)** and the cardiomyocytes within the cardiac bundles are highly anisotropic **(Figure 1b)**. In this study, we have developed a microfabricated bioreactor to generate cardiac biowires *in vitro* recapitulating the structure and function of native cardiac bundles. To the best of our knowledge, this is the first study to examine the drug effects on cardiomyocytes by perfusion within cardiac bundle model, which better mimics native myocardium mass transfer properties compared to

other engineered heart tissues. This bioreactor provided topographical cues for the cardiac cells to elongate and align, and was also integrated with other cues, e.g. electrical stimulation.

Gel compaction has been widely applied in tissue engineering to create 3D microtissue constructs for *in vivo* implantation[30] and *in vitro* models[16,31]. Compared to scaffold-based constructs, the self-assembled constructs from gel compaction produce increased force of contraction due to the higher cell density after the compaction[32]. Moreover, there is increasing interest in microtissue constructs made by gel compaction as microarrays for drug testing because they provide much higher throughput than conventional models[16,31,33,34]. In this study, type I collagen was chosen as the main gel matrix as it is one of the main ECM components of native myocardium. We noted that previous *in vitro* collagen-based models only stayed intact for several days due to their poor mechanical properties[31]. In our microfabricated system, with the mechanical support provided by the suspended templates, the cardiac biowires remained stable in the bioreactor for weeks. We were able to generate cardiac tissues in larger scale (up to 5 cm long) compared to other *in vitro* models and the dimensions of the cell culture channel could be easily customized, which could render additional control over the morphology of the cardiac biowires. The cell culture channels were initially designed to be 300 μm in height considering the limitations for oxygen and nutrient supply[35]. Moreover, the presence of the templates enabled easy disassembly of the biowire from the bioreactor and facile handling of the cardiac biowires at the end of cultivation for further characterization.

Our microfabricated bioreactor was also able to generate cardiac biowires that are 5 cm long, which is comparable to the height of the human heart. The feasibility of handling individual cardiac biowire together with the ability to create macro-scale biowires raise up the prospect of investigating the alignment of multiple cardiac biowires by bundling or weaving them together to generate thicker structures, using similar methods as described by Onoe et al[36]. To characterize the force generated by the cardiac biowires or cardiac biowire bundles, degradable sutures could be used to generate template-free cardiac biowires which will be a topic of our future studies.

To validate our microfabricated bioreactor, neonatal rat cardiomyocytes were used in preliminary studies. Only when seeded at higher cell density (> 5×10^7 cells/ml), which is comparable to the cell density in native rat myocardium (~10^8 cells/ml)[37], the cardiac biowires started spontaneous beating on day 3-4. The template provided contact guidance for the cells to elongate and align along with, recapitulating the anisotropic properties of cardiomyocytes in the native myocardium. The image analysis was done on cell nuclei due to the difficulty of defining cell membranes within 3D tissue. However, nuclear alignment is a sufficient indication of cell alignment and also one of the hallmarks of native myocardium **(Figure 1c)**.

To further develop the biowire system, we used PTFE tubing as the template instead of the 6-0 silk suture. The commercially available PTFE tubing was chosen because it is biocompatible (USP Class VI), extremely non-absorbent (ideal for drug testing), and micro-scale in dimension (ID = 50 μm, OD = 150 μm), on the order of

post-capillary venules in size[38]. Due to the small size of the inner lumen, we used negative pressure to drive the perfusion instead of positive pressure. Two microfabricated modules were added to the system to enable long-term perfusion and incubation of the biowire system. Indicated by the shortening of biowire during self-remodeling, the cell attachment on PTFE tubing was not as strong as that on silk suture, mainly because of the smoothness of the PTFE tubing surface **(Figure 4b)**. However, the cell-gel composite was still able to assemble itself around the tubing with a circular cross-section.

In this study, NO was chosen as a model drug because of following reasons: (1) NO is produced by endothelial cells in native myocardium, and then transported in the radial direction to cardiomyocytes[39], the scenario we were trying to recapitulate in our biowire bioreactor; (2) NO plays a critical role in regulating myocardial function，through both vascular-dependent and –independent effects[39]; (3) there is increasing evidence showing that NO is directly implicated in cardiomyocyte disease development and prevention, such as in ischemia-reperfusion injury[40]; (4) NO is a small gas molecular, which can readily pass the tubing wall. SNP was chosen as the NO donor because it is a common NO donor used in clinical studies[41,42]. Moreover, SNP aqueous solution was reported to release NO at a constant rate over several hours *in vitro*[43].

For the NO treatment testing, we generated human cardiac biowires from hESC-derived cardiomyocytes. The human cardiac biowire started spontaneous

beating as early as day 1 and the beating was synchronized within 7 days. After 24 hr of NO treatment, the beating frequencies of the human cardiac biowires significantly slowed down compared to their basal level. This result corresponds with the vasodilator effect of NO *in vivo*[44] and might be caused by degradation of myofibrillar cytoskeleton, which has been seen by Chiusa et al[45]. However, NO shows bi-polar inotropic effect at lower concentrations with diverse intracellular mechanisms and there were discrepancies between studies due to the lack of standardization for *in vitro* models[39]. Therefore our microfabricated bioreactor could serve as a novel platform to uncover the effects of NO on cardiomyocytes at the tissue level.

To demonstrate the versatility of our biowire bioreactors, electrical stimulation was integrated with the system as it has been reported to improve the phenotypes of cardiomyocytes[2,20]. Because the cells in the cardiac biowires were anisotropic, we studied both parallel- and perpendicular- field electrical stimulations on the rat biowires. The higher tissue stiffness under parallel electrical stimulation, which was closer to isolated neonatal rat cardiac tissue (6.8±2.8 kPa)[46], were attributed to more organized cellular contractile apparatus as characterized by immunohistochemical staining. The perfusable human cardiac biowires were electrically stimulated and perfused at the same time and this brings the prospect to study the interaction between electrical stimulation and pharmaceutical agents delivered in a physiological manner. A more detailed study on electrical stimulation alone of biowires based on human pluripotent cardiomyocytes has been done in our group and indicated that electrical stimulation of progressive frequency increase markedly improved the maturation of

hPSC-derived cardiomyocytes in terms of myofibril structure and electrical properties[19].

Medium perfusion has been recognized to improve the viability and functionality of cardiomyocytes within cardiac constructs *in vitro* since perfusion significantly improves oxygen and nutrient supply[47]. In most of previous studies, bioreactors provided medium perfusion by sandwiching cell-laden porous scaffold, while exposing the cardiomyocytes directly to the flow[47–49]. This does not exactly recapitulate the native myocardium where the blood supply flows through a dense vascular network that minimizes transport distances but also protects cardiomyocytes from shear[50]. More recently, bioreactors were developed to provide the electrical stimulation and medium perfusion simultaneously and it was shown that perfusion and stimulation had a synergistic effect on improving the contractile functionality of the cardiac constructs[51,50]. However, the cardiac constructs in these systems were based on porous scaffolds and therefore unable to provide the information about the effect of electrical stimulation on anisotropic cardiac tissue.

Previous studies describe the design of perfusion bioreactors that enable high-throughput *in vitro* drug testing on cardiac constructs[52,49]. Kaneko et al designed a microchamber array chip to evaluate single cell level interactions for drug testing[52]. Agarwal et al designed a bioreactor composed of a microarray of cantilevers that was able to characterize diastolic and systolic stresses generated by anisotropic cardiac microtissue in real-time and the bioreactor could provide electrical stimulation on

these cardiac microtissues[49]. These two studies characterized cardiac function on either single cell or monolayer level, which might be insufficient to provide accurate information of cardiac disease as in our complex native system. Moreover, the drugs investigated in these studies were directly applied to the cells, instead to the blood compartment, and the presence of flow generated shear stress on cardiomyocytes, both of which contributed to the generation of an unphysiological environment compared to that cardiomyocytes experience in the native heart.

There are several advantages of our microfabricated cardiac biowire bioreactors: (1) they are better mimic of the native cardiac bundle structure with anisotropic alignment; (2) the presence of the template enables easier handling for later characterization and keeps the entire structure stable for weeks; (3) the device could be easily customized and applicable for high-throughput drug screening; (4) the platform provides topographical stimulation by itself; (5) the platform is versatile and could be integrated with other stimuli as well (e.g. mechanical stimulation); (6) the perfusable cardiac biowire system is the first platform to study pharmacological agents applied to cardiomyocytes by perfusion through cardiac bundle mimic and could provide valuable knowledge on cardiac disease development and therapeutics.

While this perfusable cardiac biowire platform provides us many opportunities, there are still some limitations of our current platform. The permeability of the commercially available PTFE tubing renders limitation on the drug candidates that can be tested, as only small molecules can diffuse appreciably through the tubing wall

and proteins cannot. Ideal tubing materials should be microporous for better permeability. Further studies are required to investigate other relevant pharmacological agents and seeding endothelial cells in the tubing lumen to study the interaction between endothelial cells and cardiomyocytes could also be pursued.

5. Conclusions

In conclusion, we have developed a microfabricated cardiac biowire bioreactor that is capable of testing pharmacological agents applied by perfusion through the lumen. The bioreactor provides topographical cues for the cardiomyocytes to assemble and align and it could be integrated with other stimuli to further improve the phenotypes of the cardiomyocytes. The engineered cardiac biowires could serve as *in vitro* models that recapitulate the structure and function of the *in vivo* cardiac bundles for studies of cardiac development and disease.

6. Acknowledgments

The authors would like to thank Zheng Gong for his kind help with preparing Figure 3d. This work was funded by grants from Ontario Research Fund–Global Leadership Round 2 (ORF-GL2), Natural Sciences and Engineering Research Council of Canada (NSERC) Strategic Grant (STPGP 381002-09), Canadian Institutes of Health Research (CIHR) Operating Grant (MOP-126027), NSERC-CIHR Collaborative Health Research, Grant (CHRPJ 385981-10), NSERC Discovery Grant (RGPIN 326982-10), NSERC Discovery Accelerator Supplement (RGPAS 396125-10),

National Institutes of Health grant 2R01 HL076485 and Heart and Stroke Foundation grant (T6946).

References

1. A. S. Go, D. Mozaffarian, V. L. Roger, E. J. Benjamin, J. D. Berry, W. B. Borden, D. M. Bravata, S. Dai, E. S. Ford, C. S. Fox, S. Franco, H. J. Fullerton, C. Gillespie, S. M. Hailpern, J. a Heit, V. J. Howard, M. D. Huffman, B. M. Kissela, S. J. Kittner, D. T. Lackland, J. H. Lichtman, L. D. Lisabeth, D. Magid, G. M. Marcus, A. Marelli, D. B. Matchar, D. K. McGuire, E. R. Mohler, C. S. Moy, M. E. Mussolino, G. Nichol, N. P. Paynter, P. J. Schreiner, P. D. Sorlie, J. Stein, T. N. Turan, S. S. Virani, N. D. Wong, D. Woo, and M. B. Turner, *Circulation*, 2013, **127**, e6–e245.

2. M. Radisic, H. Park, H. Shing, T. Consi, F. J. Schoen, R. Langer, L. E. Freed, and G. Vunjak-Novakovic, *Proc. Natl. Acad. Sci. U. S. A.*, 2004, **101**, 18129–34.

3. W. H. Zimmermann, K. Schneiderbanger, P. Schubert, M. Didie, F. Munzel, J. F. Heubach, S. Kostin, W. L. Neuhuber, and T. Eschenhagen, *Circ. Res.*, 2002, **90**, 223–230.

4. T. Shimizu, M. Yamato, Y. Isoi, T. Akutsu, T. Setomaru, K. Abe, A. Kikuchi, M. Umezu, and T. Okano, *Circ. Res.*, 2002, **90**, e40–e48.

5. D. Sinnecker, A. Goedel, K.-L. Laugwitz, and A. Moretti, *Circ. Res.*, 2013, **112**, 961–8.

6. S. Y. Ho, *Eur. J. Echocardiogr.*, 2009, **10**, iii3–iii7.

7. P. J. Hunter, A. J. Pullan, and B. H. Smaill, *Annu. Rev. Biomed. Eng.*, 2003, **5**, 147–77.

8. B. Fermini and A. a Fossa, *Nat. Rev. Drug Discov.*, 2003, **2**, 439–47.

9. U.S. Food and Drug Administration, *Recalls, Mark. Withdrawals Saf. Alerts*, 2012.

10. J. P. Piccini, D. J. Whellan, B. R. Berridge, J. K. Finkle, S. D. Pettit, N. Stockbridge, J.-P. Valentin, H. M. Vargas, and M. W. Krucoff, *Am. Heart J.*, 2009, **158**, 317–26.

11. M. Yazawa, B. Hsueh, X. Jia, A. M. Pasca, J. A. Bernstein, J. Hallmayer, and R. E. Dolmetsch, *Nature*, 2011, **471**, 230–4.

12. A. Moretti, M. Bellin, A. Welling, C. B. Jung, J. T. Lam, L. Bott-Flügel, T. Dorn, A. Goedel, C. Höhnke, F. Hofmann, M. Seyfarth, D. Sinnecker, A. Schömig, and K.-L. Laugwitz, *N. Engl. J. Med.*, 2010, **363**, 1397–409.

13. X. Carvajal-Vergara, A. Sevilla, S. L. D'Souza, Y.-S. Ang, C. Schaniel, D.-F. Lee, L. Yang, A. D. Kaplan, E. D. Adler, R. Rozov, Y. Ge, N. Cohen, L. J. Edelmann, B. Chang, A. Waghray, J. Su, S. Pardo, K. D. Lichtenbelt, M. Tartaglia, B. D. Gelb, and I. R. Lemischka, *Nature*, 2010, **465**, 808–12.

14. N. Sun, M. Yazawa, J. Liu, L. Han, V. Sanchez-Freire, O. J. Abilez, E. G. Navarrete, S. Hu, L. Wang, A. Lee, A. Pavlovic, S. Lin, R. Chen, R. J. Hajjar, M. P. Snyder, R. E. Dolmetsch, M. J. Butte, E. A. Ashley, M. T. Longaker, R. C. Robbins, and J. C. Wu, *Sci. Transl. Med.*, 2012, **4**, 130ra47.

15. K. Shapira-Schweitzer, M. Habib, L. Gepstein, and D. Seliktar, *J. Mol. Cell. Cardiol.*, 2009, **46**, 213–24.

16. A. Hansen, A. Eder, M. Bönstrup, M. Flato, M. Mewe, S. Schaaf, B. Aksehirlioglu, A. P. Schwoerer, A. Schwörer, J. Uebeler, and T. Eschenhagen, *Circ. Res.*, 2010, **107**, 35–44.

17. E. Serena, E. Cimetta, S. Zatti, T. Zaglia, M. Zagallo, G. Keller, and N. Elvassore, *PLoS One*, 2012, **7**, e48483.

18. N. Christoforou, B. Liau, S. Chakraborty, M. Chellapan, N. Bursac, and K. W. Leong, *PLoS One*, 2013, **8**, e65963.

19. S. S. Nunes, J. W. Miklas, J. Liu, R. Aschar-Sobbi, Y. Xiao, B. Zhang, J. Jiang, S. Massé, M. Gagliardi, A. Hsieh, N. Thavandiran, M. a Laflamme, K. Nanthakumar, G. J. Gross, P. H. Backx, G. Keller, and M. Radisic, *Nat. Methods*, 2013, **10**, 781–7.

20. H. T. Heidi Au, B. Cui, Z. E. Chu, T. Veres, and M. Radisic, *Lab Chip*, 2009, **9**.

21. L. a Reis, L. L. Y. Chiu, Y. Liang, K. Hyunh, A. Momen, and M. Radisic, *Acta Biomater.*, 2012, **8**, 1022–36.

22. L. Yang, M. H. Soonpaa, E. D. Adler, T. K. Roepke, S. J. Kattman, M. Kennedy, E. Henckaerts, K. Bonham, G. W. Abbott, R. M. Linden, L. J. Field, and G. M. Keller, *Nature*, 2008, **453**, 524–8.

23. S. J. Kattman, A. D. Witty, M. Gagliardi, N. C. Dubois, M. Niapour, A. Hotta, J. Ellis, and G. Keller, *Cell Stem Cell*, 2011, **8**, 228–40.

24. F. Xu, T. Beyazoglu, E. Hefner, U. A. Gurkan, and U. Demirci, *Tissue Eng. Part C. Methods*, 2011, **17**, 641–649.

25. D. Sage, F. R. Neumann, F. Hediger, S. M. Gasser, and M. Unser, *IEEE Trans. image Process.*, 2005, **14**, 1372–83.

26. L. L. Chiu, R. K. Iyer, J. P. King, and M. Radisic, *Tissue Eng. Part A*, 2011, **17**, 1465–1477.

27. H. Liu, Y. Sun, and C. A. Simmons, *J. Biomech.*, 2013.

28. D.-H. Kim, E. A. Lipke, P. Kim, R. Cheong, S. Thompson, M. Delannoy, K.-Y. Suh, L. Tung, and A. Levchenko, *Proc. Natl. Acad. Sci.*, 2010, **107**, 565–570.

29. C. N. Hall and J. Garthwaite, *Nitric Oxide*, 2009, **21**, 92–103.

30. W.-H. Zimmermann, I. Melnychenko, G. Wasmeier, M. Didie, H. Naito, U. Nixdorff, A. Hess, L. Budinsky, K. Brune, B. Michaelis, S. Dhein, A. Schwoerer, H. Ehmke, and T. Eschenhagen, *Nat Med*, 2006, **12**, 452–458.

31. W. R. Legant, A. Pathak, M. T. Yang, V. S. Deshpande, R. M. McMeeking, and C. S. Chen, *Proc. Natl. Acad. Sci. U. S. A.*, 2009, **106**, 10097–102.

32. K. Baar, R. Birla, M. O. Boluyt, G. H. Borschel, E. M. Arruda, and R. G. Dennis, *FASEB J.*, 2005, **19**, 275–7.

33. G. Kensah, I. Gruh, J. Viering, H. Schumann, J. Dahlmann, H. Meyer, D. Skvorc, A. Bär, P. Akhyari, A. Heisterkamp, A. Haverich, and U. Martin, *Tissue Eng. Part C. Methods*, 2011, **17**, 463–73.

34. T. Boudou, W. R. Legant, A. Mu, M. A. Borochin, N. Thavandiran, M. Radisic, P. W. Zandstra, J. A. Epstein, K. B. Margulies, and C. S. Chen, *Tissue Eng. Part A*, 2012.

35. M. Radisic, J. Malda, E. Epping, W. Geng, R. Langer, and G. Vunjak-Novakovic, *Biotechnol. Bioeng.*, 2006, **93**, 332–43.

36. H. Onoe, T. Okitsu, A. Itou, M. Kato-Negishi, R. Gojo, D. Kiriya, K. Sato, S. Miura, S. Iwanaga, K. Kuribayashi-Shigetomi, Y. T. Matsunaga, Y. Shimoyama, and S. Takeuchi, *Nat. Mater.*, 2013, **12**, 584–590.

37. M. Radisic, M. Euloth, L. Yang, R. Langer, L. E. Freed, and G. Vunjak-Novakovic, *Biotechnol. Bioeng.*, 2003, **82**, 403–414.

38. M. P. Wiedeman, *Circ. Res.*, 1963, **12**, 375–8.

39. P. B. Massion, O. Feron, C. Dessy, and J.-L. Balligand, *Circ. Res.*, 2003, **93**, 388–98.

40. E. T. Chouchani, C. Methner, S. M. Nadtochiy, A. Logan, V. R. Pell, S. Ding, A. M. James, H. M. Cochemé, J. Reinhold, K. S. Lilley, L. Partridge, I. M. Fearnley, A. J. Robinson, R. C. Hartley, R. a J. Smith, T. Krieg, P. S. Brookes, and M. P. Murphy, *Nat. Med.*, 2013, **19**.

41. R. R. Miller, L. A. Vismara, R. Zelis, E. A. Amsterdam, and D. T. Mason, *Circulation*, 1975, **51**, 328–36.

42. W. Mullens, Z. Abrahams, G. S. Francis, H. N. Skouri, R. C. Starling, J. B. Young, D. O. Taylor, and W. H. W. Tang, *J. Am. Coll. Cardiol.*, 2008, **52**, 200–7.

43. L. Ederli, L. Reale, L. Madeo, F. Ferranti, C. Gehring, M. Fornaciari, B. Romano, and S. Pasqualini, *Plant Physiol. Biochem.*, 2009, **47**, 42–8.

44. M. Seddon, A. M. Shah, and B. Casadei, *Cardiovasc. Res.*, 2007, **75**, 315–26.

45. M. Chiusa, F. Timolati, J. C. Perriard, T. M. Suter, and C. Zuppinger, *Eur. J. Histochem.*, 2012, **56**, e15.

46. B. Bhana, R. K. Iyer, W. L. K. Chen, R. Zhao, K. L. Sider, M. Likhitpanichkul, C. A. Simmons, and M. Radisic, *Biotechnol. Bioeng.*, 2010, **105**, 1148–60.

47. M. Radisic, H. Park, F. Chen, J. E. Salazar-Lazzaro, Y. Wang, R. Dennis, R. Langer, L. E. Freed, and G. Vunjak-Novakovic, *Tissue Eng*, 2006, **12**, 2077–2091.

48. M. Radisic, L. Yang, J. Boublik, R. J. Cohen, R. Langer, L. E. Freed, and G. Vunjak-Novakovic, *Am. J. Physiol. Heart Circ. Physiol.*, 2004, **286**, H507–16.

49. A. Agarwal, J. A. Goss, A. Cho, M. L. McCain, and K. K. Parker, *Lab Chip*, 2013, **13**, 3599–3608.

50. R. Maidhof, N. Tandon, E. J. Lee, J. Luo, Y. Duan, K. Yeager, E. Konofagou, and G. Vunjak-Novakovic, *J. Tissue Eng. Regen. Med.*, 2012, **6**, e12–23.

51. Y. Barash, T. Dvir, P. Tandeitnik, E. Ruvinov, H. Guterman, and S. Cohen, *Tissue Eng. Part C. Methods*, 2010, **16**, 1417–26.

52. T. Kaneko, K. Kojima, and K. Yasuda, *Analyst*, 2007, **132**, 892–8.

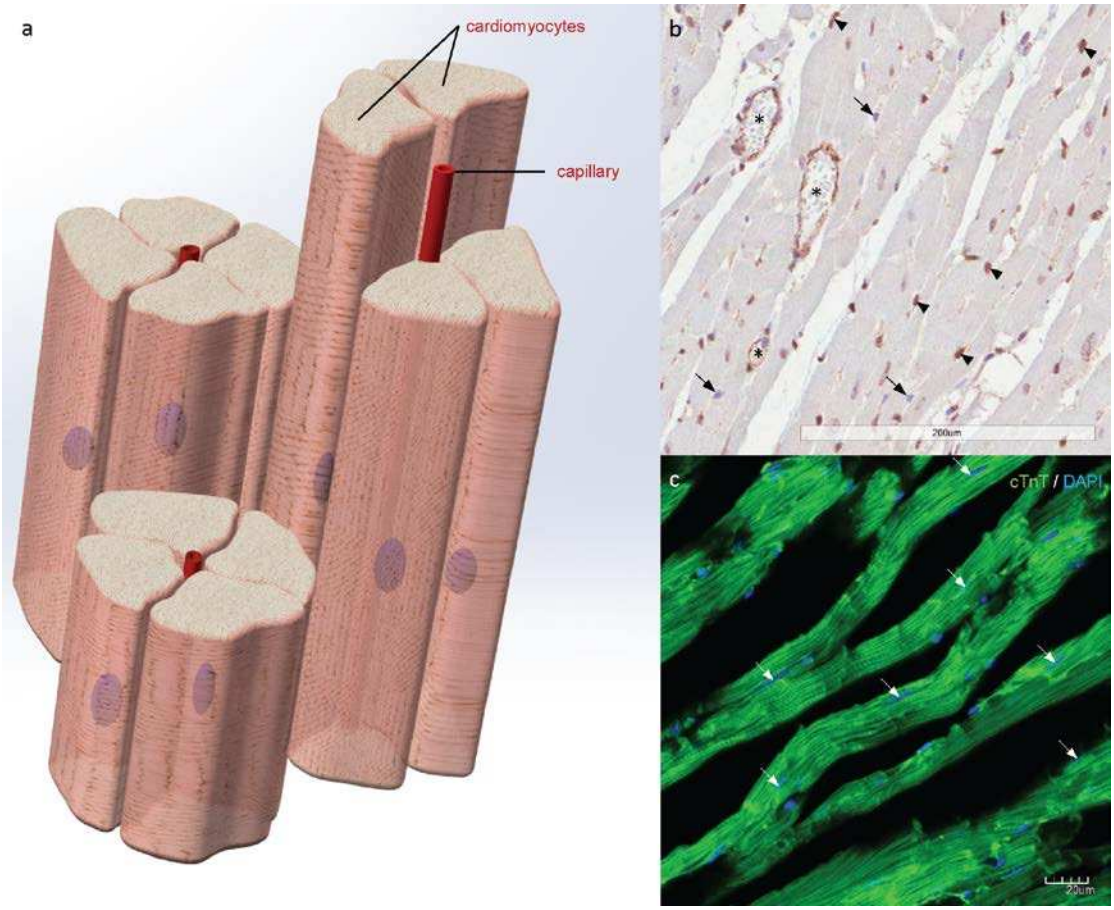

Figure 1. Cardiac bundles in native myocardium. (a) Schematic illustration of the structure of cardiac bundles in native myocardium. Cardiomyocytes are elongated, aligned, and grouped into bundles around capillaries. **(b)** Tangential section of adult rat myocardium with CD31 staining (brown). Nuclei were counterstained as light violet (long arrows). The blood vessels were noted as asterisks while the capillaries were noted as short arrows. **(c)** Fluorescent image of tangential cryosection of neonatal rat myocardium. Cardiac troponin T (cTnT) was stained against Alexa 488-labeled (green) antibody, showing its unique striation structure. Cell nuclei were counterstained with DAPI (blue) and the long arrows indicate elongated nuclei.

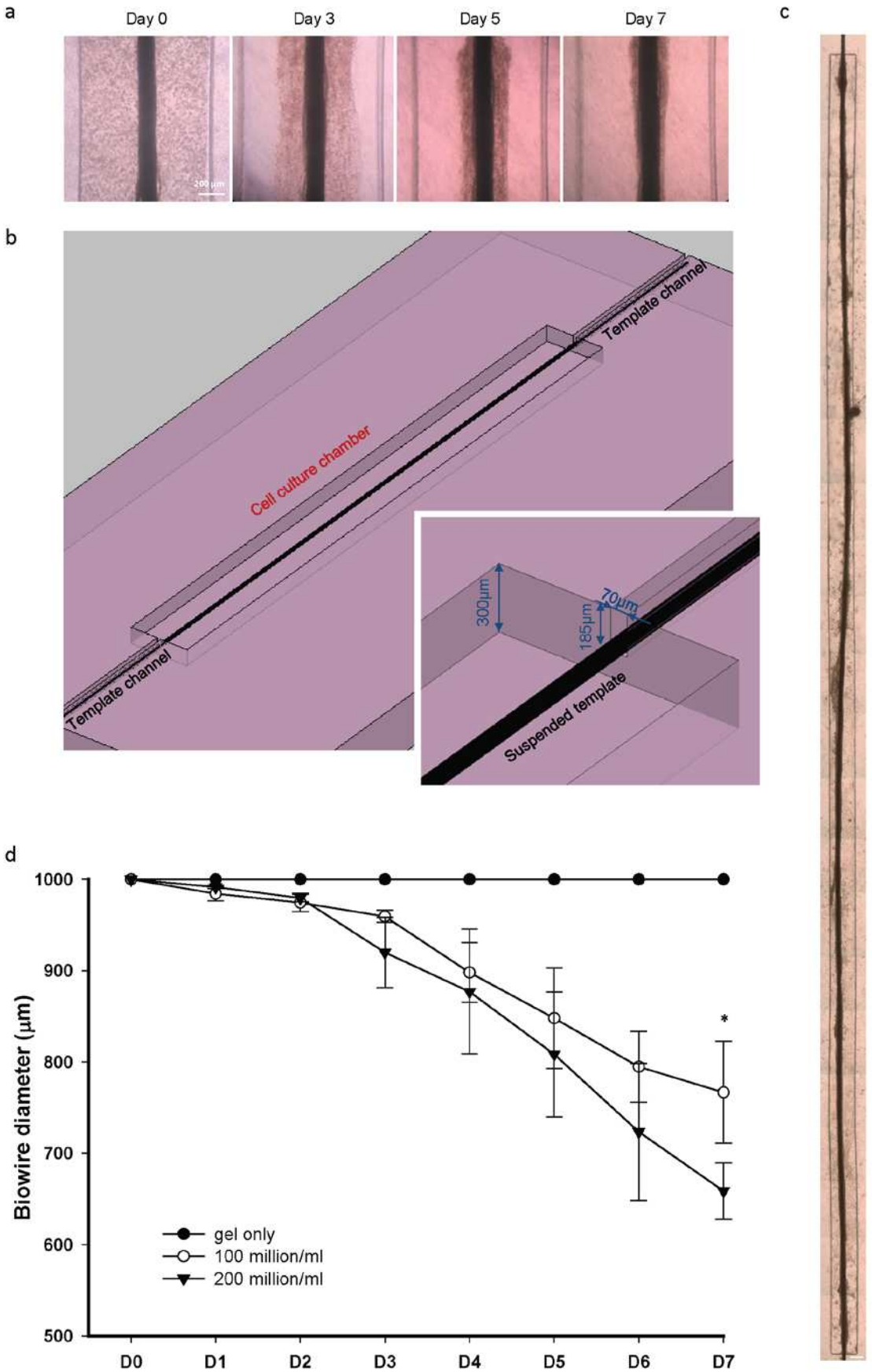

Figure 2. Generation of cardiac biowires with microfabricated bioreactor. (a) Within 7 days of cultivation, neonatal rat cardiomyocytes (8.75 million cells/ml) remodeled the gel and compacted around the suture template to form the biowire structure. **(b)** Device design of the microfabricated bioreactor with suspended 6-0 suture template. **(c)** A customized ultra-long cardiac biowire in the length of 5 cm (scale bar = 500 μm). **(d)** Quantification of gel compaction and its dependence on initial seeding density of cardiomyocytes (mean ± SD, n = 3). With no cardiomyocytes seeded (gel only), the gel did not compact and form biowire structure. Biowires with higher seeding density (200 million cells/ml) compacted faster than those with lower seeding density (100 million cells/ml) during the remodelling.

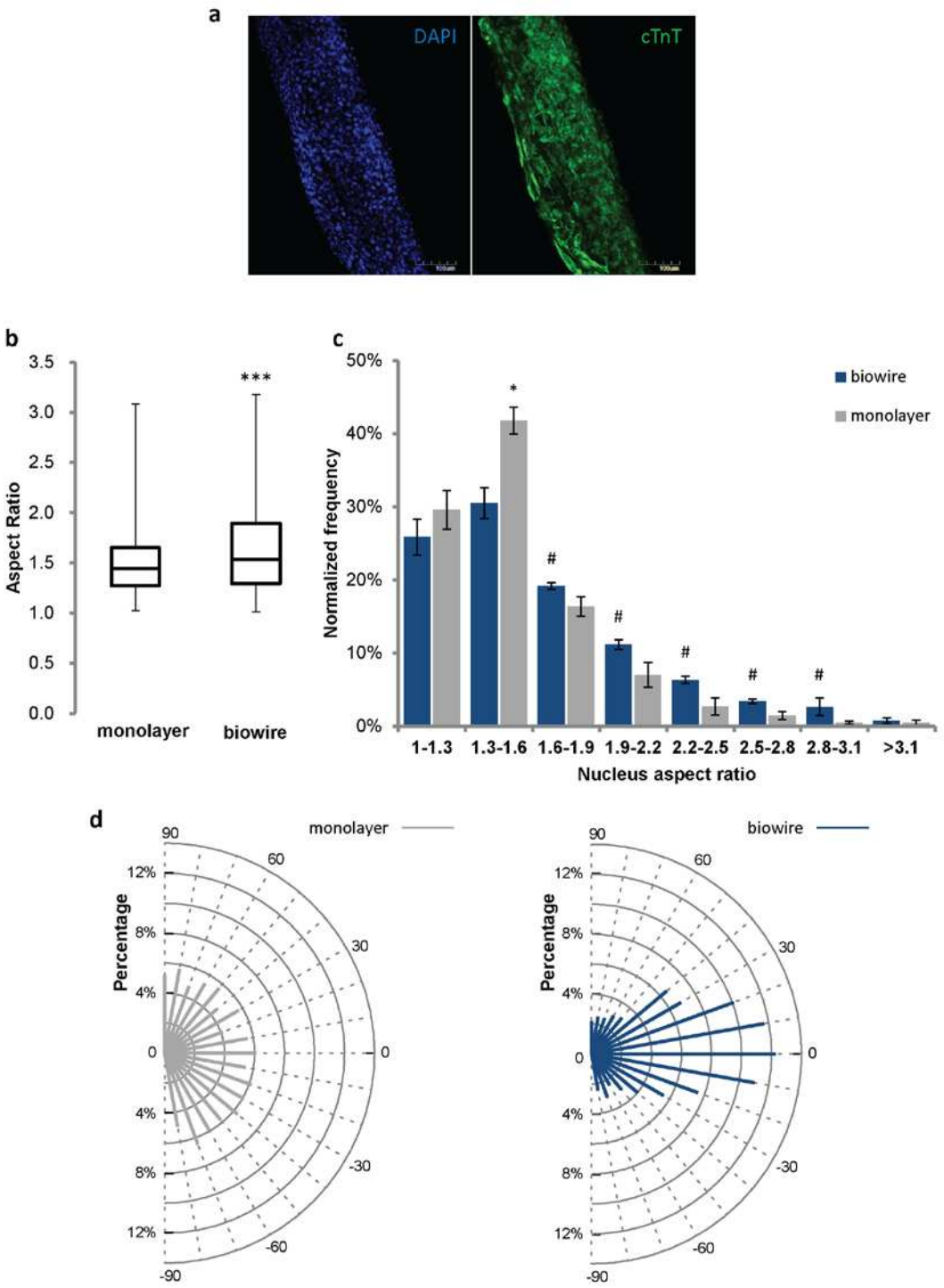

Figure 3. The suture template provides topographical cues in the biowires for the cardiomyocytes to elongate and align. (a) Confocal images of the biowire with nuclei counterstained with DAPI and cardiac Troponin-T (cTnT) stained with Alexa 488 (green). **(b)** Nuclei aspect ratios (~1000 nuclei characterized per sample) of cardiac cells cultured as monolayer vs. seeded in the biowires plotted in box plot showing the 1st quartile, median, and 3rd quartile with a significant difference between two groups (***, $p < 0.001$). **(c)** Histogram showing the distribution of nuclei aspect ratios of biowire group and monolayer group (n = 3 per group). There were significantly higher frequencies in the lower aspect ratio range in monolayer group (*,

p < 0.05) and higher frequencies in higher aspect ratio range in biowire group (#, p < 0.05). **(d)** Characterization of nucleus orientation reveals random distribution of nuclei in the monolayer group (random direction as 0°) and oriented distribution of nuclei along with the suture template in the biowire group (orientation of suture template as 0°). Dashed lines indicate orientation angle, solid hemi-circular lines indicate the percentage gridlines, and grey (monolayer) or blue (biowire) lines indicate the actual percentage of the nuclei in the specific orientation angle.

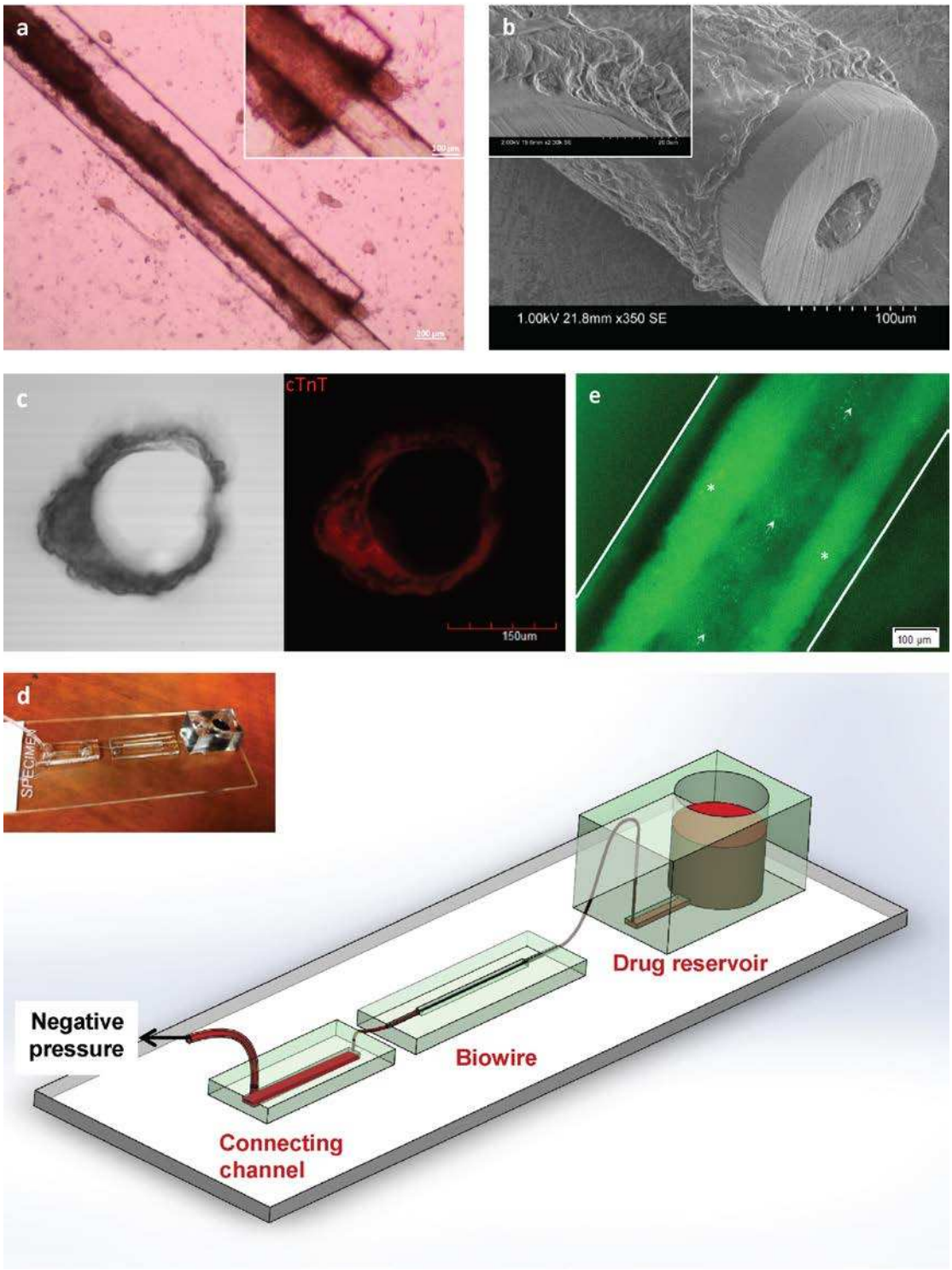

Figure 4. Generation of perfusable cardiac biowires. (a) Neonatal rat cardiomyocytes (200 million cells/ml) remodeled the gel and compacted around the tubing template (ID = 50.8 µm, OD = 152.4 µm). A close-up view showing the tubing lumen at the end of the biowire is given at top-right. **(b)** SEM images demonstrate that the cardiac tissue attached to the tubing surface and formed a uniform-thick layer after remodelling. **(c)** Representative phase contrast image (left) and confocal image (right) showing the circular morphology of the cross section of the perfusable cardiac biowire with the expression of cardiac Troponin-T (cTnT). **(d)** Set-up of the perfusion

device. Two microfabricated modules were added to the bioreactor system: a drug reservoir at one end of the biowire and a channel at the other end for connection to an external negative pressure source. The entire biowire perfusion system was bonded on a glass slide (real-life image shown at the top-left corner). **(e)** The tubing-templated biowire was perfused with FITC-labeled polystyrene beads (1 μm in diameter). Dash lines illustrate the wall of the cell culture channel. FITC-labeled beads were indicated by arrows. Asterisks indicate the auto fluorescence from the cardiomyocytes within the cardiac biowire. This image was over-exposed to better visualize the fluorescent beads.

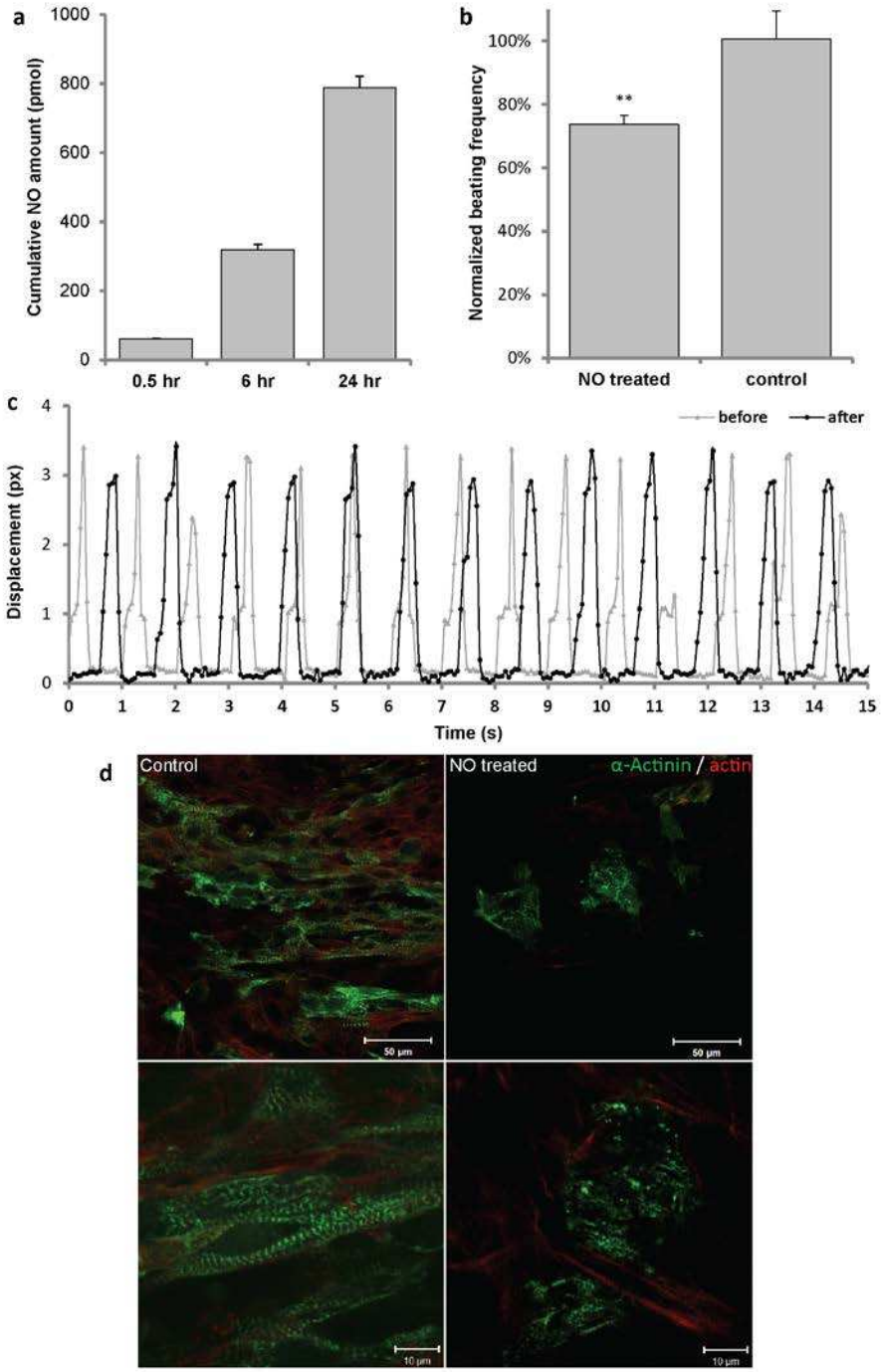

Figure 5. Nitric oxide (NO) treatment on human tubing-templated biowires. (a) Quantification of NO amount passing through the tubing wall after perfusing SNP (200 mM) for 0.5 hr, 6 hr, and 24 hr. **(b)** 24 hr NO treatment significantly slowed down the beating of biowires compared to the basal levels while there was no significant change in the non-treated biowires (n = 3 per group, $p < 0.01$). **(c)** Quantified by image analysis, the beating rate of a biowire after 24 hr NO treatment was less frequent compared to the basal level. **(d)** Confocal images showing the disrupted α-actinin (green) structure within the NO-treated biowire (right) compared to the control (left) (top: lower magnification; bottom: higher magnification).

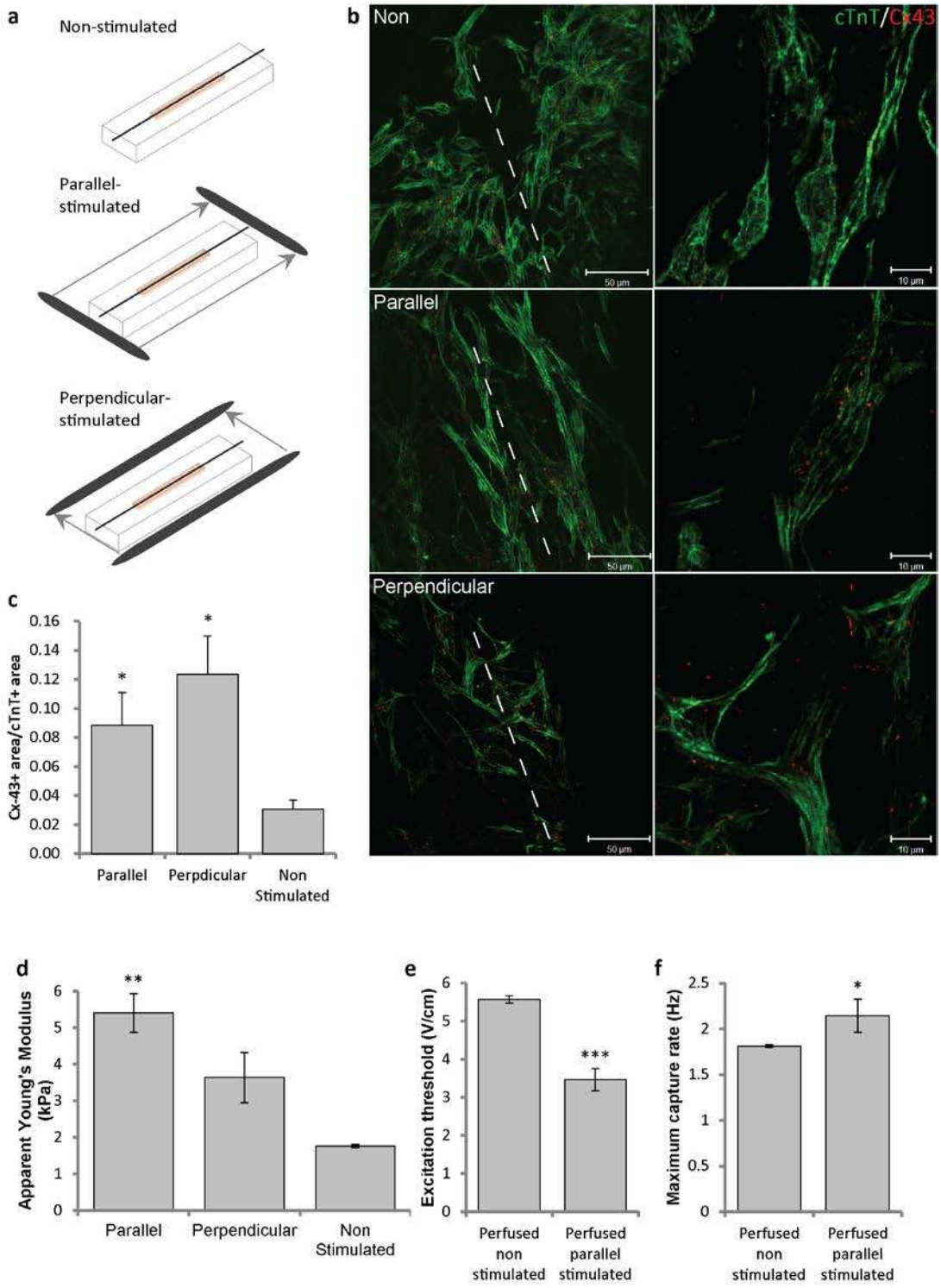

Figure 6. Electrical stimulation and perfusion of cardiac biowires. (a) Experimental set-up of biowires under different electrical stimulation conditions. Carbon rods (in black) connected to an external stimulator provided either parallel or perpendicular electrical field stimulation on cardiac biowires for 4 days starting on Day 4. **(b)** Representative confocal images of biowires after application of different electrical stimulation conditions (left: lower magnification; right: higher magnification). Parallel-stimulated biowires showed more cTnT positive (green) structures oriented along with the suture template (indicated by dashed lines). (c)

Higher ratio of Cx-43 positive area over cTnT positive area indicated stronger expression of Cx-43 in both parallel- and perpendicular-stimulated biowires compared to the non-stimulated controls ($n = 4$ per group, $p < 0.05$). **(d)** Young's modulus of cardiac biowires characterized by AFM reveals that the parallel-stimulated biowires had improved mechanical properties compared to the control biowires (**, $p < 0.01$). **(e)** Electrically stimulated perfused biowires based on hESC derived cardiomyocytes had lower excitation threshold compared to the non-stimulated controls (***, $p < 0.001$). **(f)** The electrically stimulated perfused biowires based on hESC derived cardiomyocytes had higher maximum capture rate compared to the non-stimulated controls (*, $p < 0.05$).

Video 1: Biowires based on neonatal rat cardiomyocytes started to beat spontaneously and synchronously between day 3 and day 4 post seeding, depending on the initial seeding density. Combined video shows biowires seeded with 1×10^8 cells/ml or 2×10^8 cells/ml neonatal rat cardiomyocytes on day 5 (10× magnification).

Video 2: Bright field video of perfusable biowire based on neonatal rat cardiomyocytes that was beating spontaneously on day 8 and perfused with FITC-labeled beads (diameter = 1 μm) simultaneously (10× magnification).

Video 3: Biowires based on hESC derived cardiomyocytes (labeled with eGFP) started to beat spontaneously and synchronously between day 2 and day 3 post seeding. Video shows the biowire based on hESC derived cardiomyocytes on day 6 with green fluorescent (4× magnification).

Video 4: Bright field video of the identical biowire in Video 3 at the same location (4× magnification).

Video 5: NO released from SNP that perfused through the lumen slowed down the spontaneous beating of biowires based on hESC derived cardiomyocytes. Combined video shows the spontaneous beating of the biowire before treatment (on day 7) and after 24 hr of NO treatment (10× magnification).